12R-lipoxygenase deficiency disrupts epidermal barrier function

Nikolas Epp,[1] Gerhard Fürstenberger,[1] Karsten Müller,[1] Silvia de Juanes,[1] Michael Leitges,[2] Ingrid Hausser,[3] Florian Thieme,[4] Gerhard Liebisch,[4] Gerd Schmitz,[4] and Peter Krieg[1]

[1]Section Eicosanoids and Tumor Development, German Cancer Research Center, D-69120 Heidelberg, Germany
[2]The Biotechnology Centre of Oslo, University of Oslo, N-0317, Oslo, Norway
[3]Dermatological Department, University Clinic Heidelberg, D-69115 Heidelberg, Germany
[4]Institute of Clinical Chemistry, University of Regensburg, D-93042 Regensburg, Germany

12R-lipoxygenase (12R-LOX) and the epidermal LOX-3 (eLOX-3) constitute a novel LOX pathway involved in terminal differentiation in skin. This view is supported by recent studies showing that inactivating mutations in 12R-LOX and eLOX-3 are linked to the development of autosomal recessive congenital ichthyosis. We show that 12R-LOX deficiency in mice results in a severe impairment of skin barrier function. Loss of barrier function occurs without alterations in proliferation and stratified organization of the keratinocytes, but is associated with ultrastructural anomalies in the upper granular layer, suggesting perturbance of the assembly/extrusion of lamellar bodies. Cornified envelopes from skin of 12R-LOX–deficient mice show increased fragility. Lipid analysis demonstrates a disordered composition of ceramides, in particular a decrease of ester-bound ceramide species. Moreover, processing of profilaggrin to monomeric filaggrin is impaired.

This study indicates that the 12R-LOX–eLOX-3 pathway plays a key role in the process of epidermal barrier acquisition by affecting lipid metabolism, as well as protein processing.

Introduction

Lipoxygenases (LOXs) represent a widely distributed family of nonheme, nonsulfur, iron-containing dioxygenases that catalyze the regioselective and stereoselective dioxygenation of fatty acid substrates containing one or more (Z,Z)-1,4-pentadiene moieties (Brash, 1999). Within the mammalian LOX family, a distinct subclass of epidermis-type LOX has been characterized that are preferentially expressed in skin and few other epithelial tissues (Krieg et al., 2002). They include the human 15-LOX-2 and its mouse orthologue 8-LOX, 12R-LOX, and eLOX-3. Their genes map close together within a gene cluster on human chromosome 17p13.1 that was found highly conserved within a syntenic region at the central region of mouse chromosome 11 (Krieg et al., 2001). Although exhibiting a rather heterogeneous regio- and stereospecificity, the epidermis-type LOX are phylogenetically closely related, sharing ~50% amino acid identity. Their differentiation-dependent expression pattern in epithelial tissues suggests a common physiological role in the regulation of proliferation and differentiation of epithelial cells, especially keratinocytes.

The epidermal 12R-LOX and eLOX-3 differ from all other mammalian LOX in their unique structural and enzymatic features (Boeglin et al., 1998; Krieg et al., 1999; Kinzig et al., 1999). Both proteins contain an extra domain located at the surface of the catalytic subunit. 12R-LOX represents the only mammalian LOX that forms products with R-chirality, and, unlike all other LOX, eLOX-3 does not exhibit dioxygenase activity, but functions as a hydroperoxide isomerase (Yu et al., 2003). Both enzymes act in sequence to convert arachidonic acid via 12R-hydroperoxyeicosatetraenoic acid (12R-HPETE) to the corresponding hepoxilin-like epoxyalcohol, 8R-hydroxy-11R,12R-epoxyeicosatrienoic acid. This sequence has been hypothesized to be part of a novel LOX pathway in skin that plays an important role in terminal differentiation (Jobard et al., 2002; Yu et al., 2003).

Recent genetic studies have identified mutations in the coding regions of 12R-LOX and eLOX-3 genes in patients with autosomal recessive congenital ichthyosis (ARCI), linking for the first time mutations of a LOX gene to the development of a disease (Jobard et al., 2002; Eckl et al., 2005). ARCI is a clinically and genetically heterogeneous group of skin disorders that is associated with hyperkeratosis and impaired skin barrier

Correspondence to Peter Krieg: p.krieg@dkfz.de

Abbreviations used in this paper: ARCI, autosomal recessive congenital ichthyosis; CE, cornified envelope; E, embryonic day; eLOX-3, epidermis-type LOX-3; ES, embryonic stem; HPETE, hydroperoxyeicosatetraenoic acid; LOX, lipoxygenase; PPAR, peroxisome proliferator-activated receptor; TEWL, transepidermal water loss.

The Journal of Cell Biology, Vol. 177, No. 1, April 9, 2007 173–182
http://www.jcb.org/cgi/doi/10.1083/jcb.200612116

functions (Traupe, 1989). We and others recently showed that the point mutations found in the LOX genes of the ARCI patients completely eliminated the catalytic activity of the LOX enzymes, indicating that mutational inactivation of either 12R-LOX or eLOX-3 is causally linked to the ARCI phenotype (Eckl et al., 2005; Yu et al., 2005).

To investigate the physiological role of 12R-LOX and to analyze the molecular mechanisms that underlie the ichthyosiform skin phenotype, we developed mice with targeted inactivation of the 12R-LOX gene. Examination of the resulting phenotype has revealed a crucial role of 12R-LOX in the development of epidermal barrier function, demonstrating for the first time an indispensable function of a LOX isoform for postnatal survival of mice.

Results

Generation of 12R-LOX–deficient mice

For targeting the *Alox12b* gene, we used the Cre-loxP system. A targeting vector was constructed by placing a resistance cassette flanked by loxP sites into intron 7 of *Alox12b*. A third loxP site was inserted downstream of exon 8 (Fig. 1 A). This exon encodes a highly conserved region containing two of the iron-binding histidines that are absolutely required for LOX catalytic activity (Brash, 1999; Krieg et al., 1999). Thus, Cre-mediated excision of this region yields a nonfunctional protein. The targeting construct was electroporated into E14 embryonic stem (ES) cells, followed by G418 selection. Two ES cell clones had correctly recombined alleles and were used to generate germline chimeras. Heterozygous floxed mice ($Alox12b^{+/flox}$) were mated with CMV-Cre deleter mice (Schwenk et al., 1995) to validate our construct and to generate mice harboring a disrupted *Alox12b* allele. Correct recombination and complete excision of the resistance cassette and exon 8 were confirmed by PCR analysis and Southern blot analysis, yielding the expected BamHI fragments (Fig. 1, B–D). Heterozygous $Alox12b^{+/-}$ mice were intercrossed to generate homozygous mutant mice. Genotype analysis of 112 newborns from 19 intercrosses demonstrated that wild-type, heterozygous, and homozygous mutant mice were produced in the expected Mendelian ratios, indicating no embryonic lethality of the $Alox12b^{-/-}$mice.

RT-PCR and Western blot analysis demonstrated the expression of 12R-LOX RNA and protein in skin isolated from neonatal mice. The mutated *Alox12b* RNA lacking exon 8 was expressed in heterozygous and homozygous newborn mice, and no wild-type RNA was detected in skin from homozygous mutant mice (Fig. 2 A). Wild-type 12R-LOX protein was detected in epidermis of wild-type and heterozygous mice, but was absent in the skin of homozygous $Alox12b^{-/-}$ mice. A predicted truncated 12R-LOX was not detectable, indicating translational suppression or instability of the mutated protein (Fig. 2 B). The lack of 12R-LOX protein expression in the skin of homozygous

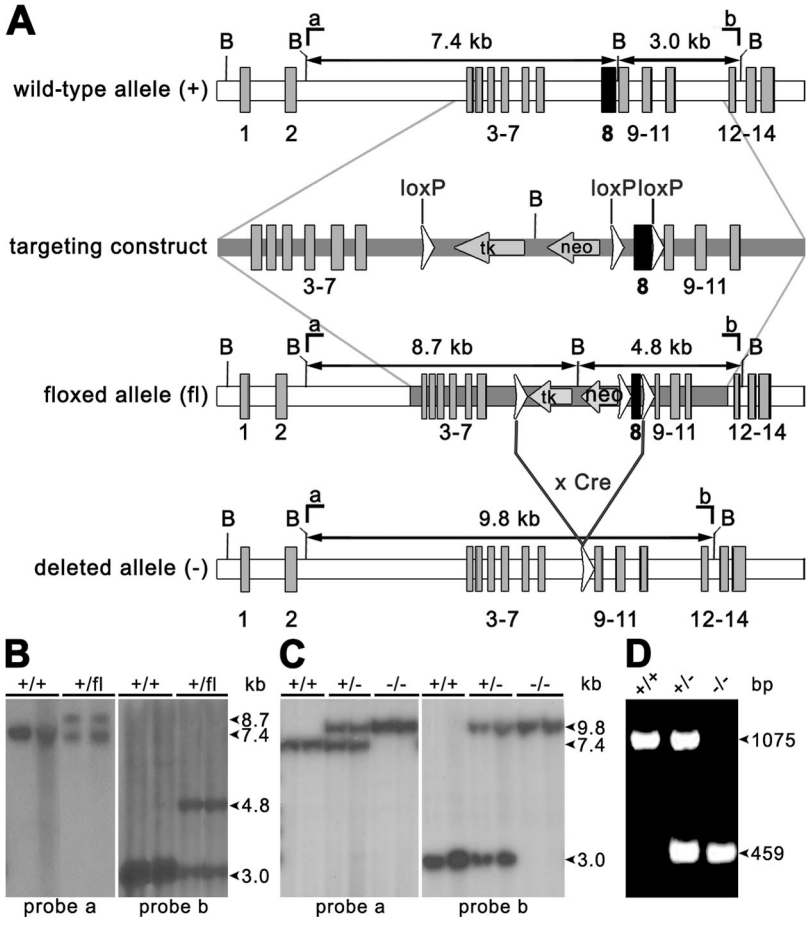

Figure 1. **Generation of 12R-LOX–deficient mice.** (A) Strategy of *Alox12b* gene targeting. B, BamHI; neo, the neomycin phosphotransferase gene; tk, the thymidine kinase gene. LoxP sites are depicted as open triangles. Probes a and b were used to identify recombinant and deleted alleles. (B) Southern blot analysis of BamHI-digested DNA from wild-type (+/+) mice (lanes 1 and 5), from ES cells (lanes 2 and 6), and from heterozygous mice (lanes 3, 4, 7, and 8) carrying the floxed allele (+/fl). Detection of an 8.7-kb fragment using probe a (left) and a 4.8-kb fragment using probe b (right) revealed the presence of the correct recombinated allele. (C) Southern blot analysis of BamHI-digested DNA from wild-type (+/+), heterozygous (+/−), and homozygous (−/−) mice carrying the floxed-deleted allele. Detection of a 9.8-kb fragment using probe a (left) and probe b (right) revealed the correct excision of the resistance cassette and exon 8. (D) PCR genotype analysis of tail DNA. Primer combination ol1231/ol709 was used, amplifying a 1,075-bp product of the wild type and a 459-bp product of the deleted allele.

mutant mice was confirmed by immunofluorescence. Using a 12R-LOX–specific mAb, a prominent and specific staining throughout the plasma membranes of keratinocytes in the stratum granulosum was seen in wild-type mice, but was absent in the homozygous mutant mice (Fig. 2 C).

Loss of skin barrier function in 12R-LOX–deficient mice

Heterozygous *Alox12b*$^{+/-}$ mice were phenotypically indistinguishable from wild-type mice and reproduced normally. At birth, *Alox12b*$^{-/-}$ mice were hard to distinguish from wild-type and heterozygous littermates upon macroscopic inspection. However, their skin soon began to develop a red, shiny appearance and became somewhat sticky to the touch (Fig. 3 A). The neonates did not feed and became progressively dehydrated. All homozygous mutant mice died within 3–5 h after birth.

The macroscopic appearance and the early neonate death of the mice suggested a perturbed water barrier. Weighing experiments showed that homozygous *Alox12b*$^{-/-}$ mice lost ~30% of their body weight within 3 h, whereas their heterozygous and wild-type littermates maintained their weight (Fig. 3 B). Transepidermal water loss (TEWL) of homozygous mutant mice was increased by a factor of ~8 compared with wild-type and heterozygous littermates (Fig. 3 C). Thus, the lethal phenotype of the 12R-LOX–deficient mice most likely resulted from water loss as a result of impaired epidermal barrier function.

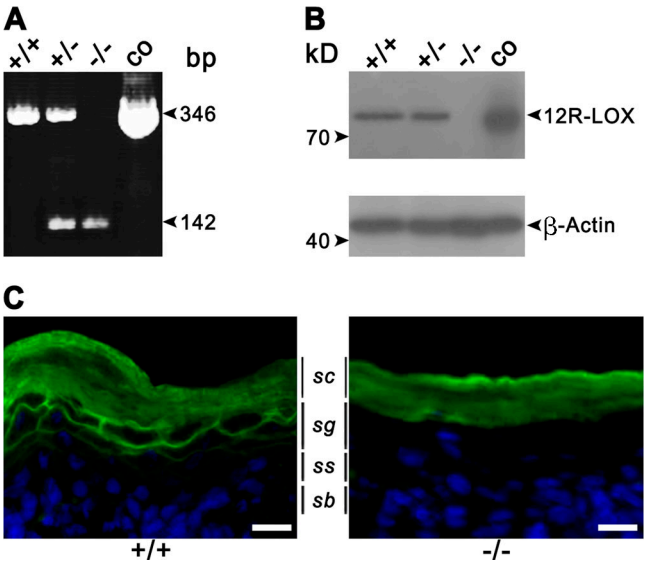

Figure 2. **The targeted deletion in the *Alox12b*-gene generates a null mutation.** (A) Detection of wild-type and mutant 12R-LOX mRNA in neonatal skin by RT-PCR. Primer combination ol230/ol709 was used to amplify a 346-bp product of the wild type and a 142-bp product of the deleted allele. (B) Loss of 12R-LOX protein in neonatal skin of 12R-LOX$^{-/-}$ mice examined by Western blot analysis using a polyclonal antiserum raised against a 12R-LOX–specific peptide (top). As a control, the cell lysate of HEK 293 transfectants exogenously expressing m12R-LOX was used. An antibody recognizing actin was used as a control for equal loading (bottom). (C) In wild-type mice, immunostaining using a 12R-LOX–specific mAb shows prominent staining of the plasma membranes of the keratinocytes in the granular layers subjacent to the stratum corneum. In 12R-LOX$^{-/-}$ mice, these structures appear negative for such a staining. Nuclei are counterstained with Hoechst 33258. sc, stratum corneum; sg, stratum granulosum; ss, stratum spinosum; sb, stratum basale. Bars, 20 μm.

Barrier formation that starts around E16 in a patterned fashion (Hardman et al., 1998) was measured with a whole-mount skin toluidine blue penetration assay. In wild-type animals, the staining pattern reflects the decrease of skin permeability from embryonic day (E) 16.5 to E17.5, when the barrier development proceeds in a dorsal to ventral pattern, up to E18.5, which is when skin has become completely impermeable. Skin of homozygous mutant mice, in contrast, remained permeable, as indicated by intense staining (Fig. 4 A). We then assessed the permeability of the newborn epidermal barrier from outside using the fluorescent dye Lucifer yellow. In skin of 12R-LOX–deficient mice, the dye was found to penetrate throughout the stratum corneum, whereas it was retained in the very top layers in the skin of wild-type mice (Fig. 4 B). These findings clearly indicate that both the inside-out and the outside-in water barrier function were severely affected in the epidermis of 12R-LOX–deficient mice. We also assessed the barrier function of tight junctions by injecting newborn mice subcutaneously with biotin and measuring its diffusion into the epidermis. Prevention of diffusion was observed in the upper granular cells of the skin of homozygous mutant mice, as well as in wild-type mice, indicating that 12R-LOX deficiency did not affect the barrier function of tight junctions (unpublished data).

Defective processing of profilaggrin to filaggrin monomers

The epidermis of newborn *Alox12b*$^{-/-}$ mice did not exhibit overt abnormalities in the stratified organization of keratinocytes

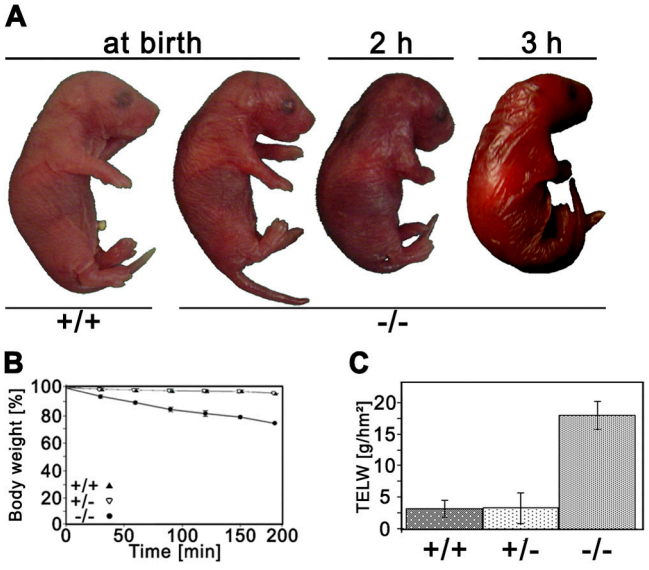

Figure 3. **Impairment of the epidermal barrier in 12R-LOX$^{-/-}$ mice.** (A) Macroscopic appearance of wild-type and 12R-LOX$^{-/-}$ mice at birth, and 2 and 3 h after birth. Note the red, shiny skin and the dehydrated appearance of 12R-LOX$^{-/-}$ mice. (B) Dehydration assay over time. Data are presented as the percentage of initial body weight in wild-type (+/+, n = 6), heterozygous (+/−, n = 9), and homozygous (−/−, n = 11) mutant mice. Only homozygous mutant showed a 10% weight loss/h. (C) TEWL assay measured on ventral surface of newborn wild-type (+/+, n = 9), heterozygous (+/−, n = 18), and homozygous (−/−, n = 15) mutant mice.

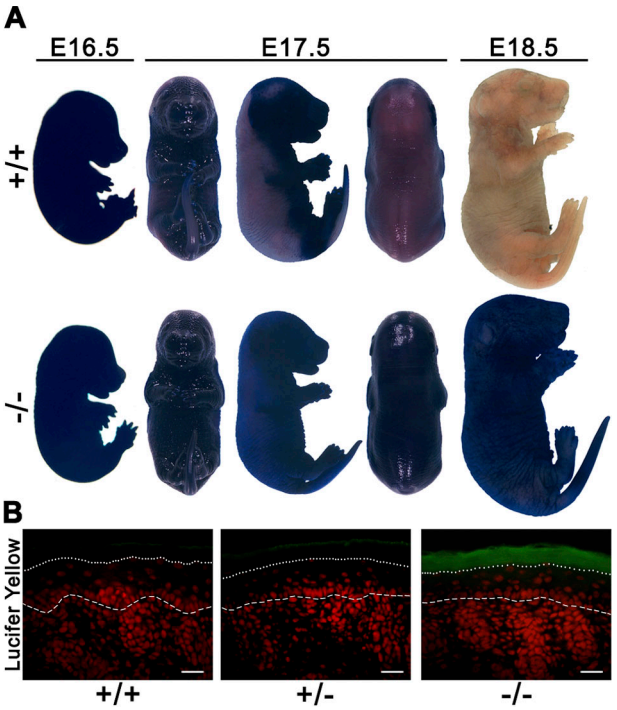

Figure 4. **Defective development of skin permeability barrier in 12R-LOX$^{-/-}$ mice.** (A) Barrier-dependent dye exclusion assay on wild-type and 12R-LOX$^{-/-}$ mice at the ages indicated. In control embryos, a decrease in skin permeability was observed from E16.5 to E17.5 as the barrier is acquired in the dorsal to ventral pattern, whereas 12R-LOX$^{-/-}$ embryos remained completely stained. (B) Lucifer yellow dye penetration assay of newborn wild-type and 12R-LOX$^{-/-}$ mice. Dye penetration (green fluorescence) across the stratum corneum was observed in skin of 12R-LOX$^{-/-}$ mice, but not in controls. Sections were counterstained with propidium iodide (red fluorescence). The dotted line shows the border of stratum corneum–stratum granulosum, the dashed line shows the epidermal–dermal junction. Bars, 20 μm.

at the level of hematoxylin and eosin–stained paraffin section images (Fig. 5). No substantial differences were observed in the basal, spinous, or granular layers. The stratum corneum, however, appeared to be more tightly packed compared with that of control skin. To unveil defects in differentiation, we analyzed the level of expression and distribution of terminal differentiation markers. Western blot analysis revealed that the levels of keratin 5 and 10, loricrin, and involucrin were not altered in the *Alox12b*-null versus control mice (Fig. 6). However, a complete loss of filaggrin monomer in knockout epidermis was associated with enhanced levels of proteolytically derived intermediates, indicating that proteolytic processing of profilaggrin was impaired. On the other hand, immunofluorescence showed a comparable distribution of the filaggrin expression in both genotypes. Similarly, other markers for epidermal differentiation, such as repetin and desmosomal proteins (claudin and occludin), revealed staining profiles that did not differ between the 12R-LOX–deficient mice and their wild-type counterparts (unpublished data). Immunofluorescence analysis indicated absence of the hyperproliferative keratin 6. Accordingly, the proliferation index as determined by Ki67 staining was also unchanged (45.4 ± 3.2% vs. 46.4 ± 0.6% in control and knockout mice, respectively). This indicates that basal cell proliferation was unaffected. The structure of the hair follicles also seemed to be normal.

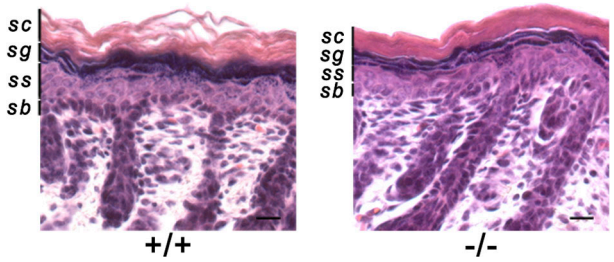

Figure 5. **Histological analysis of 12R-LOX$^{-/-}$skin.** Representative skin sections from newborn wild-type and 12R-LOX$^{-/-}$ littermates stained with hematoxylin and eosin. Staining shows a more tightly packed SC, but an otherwise normal stratified organization of keratinocytes in knockout skin. sc, stratum corneum; sg, stratum granulosum; ss, stratum spinosum; sb, stratum basale. Bars, 20 μm.

Structural abnormalities in skin of 12R-LOX–deficient mice

Histological analysis of methylene blue–stained semithin sections revealed obvious structural anomalies in the skin of the homozygous mutant mice (Fig. 7, A–C). Numerous vacuole-like structures were observed in the upper granular layers of the epidermis underlying the stratum corneum. The vesicles were variable in size and irregularly distributed. Ultrathin section EM confirmed these findings at higher resolution (Fig. 7, D–L). Although no gross differences could be detected in the horny layers of the skin from the *Alox12b*$^{-/-}$ mice, the cells of the

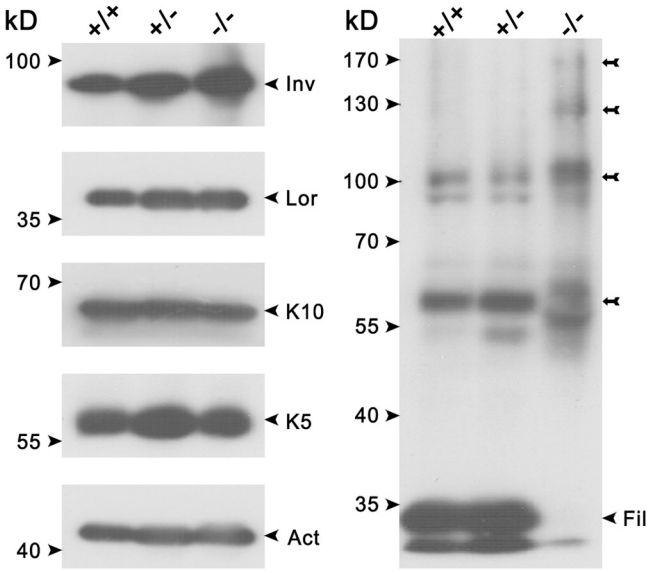

Figure 6. **Aberrant processing of profilaggrin.** Equal amounts of protein extracts from wild-type (+/+), heterozygous (+/−), and homozygous mutant (−/−) epidermis were separated trough SDS-PAGE and subjected to Western blot analysis using specific antibodies against keratin 10 (K10), keratin 5 (K5), loricrin (Lor), β-actin (Act), filaggrin (Fil), and involucrin (Inv). Note the aberrant profilaggrin–filaggrin processing in the knockout epidermis with the complete loss of the filaggrin monomers and the accumulation of proteolytically derived intermediates (arrows).

granular layer regularly contained vesicular structures of variable sizes (Fig. 7 E, asterisks). Sometimes they seemed to have fused. Most vesicles were electron-lucent with some smaller vesicles inside (Fig. 7, I and K). At higher magnifications, we could observe lamellar structures adhering to the surrounding membrane (Fig. 7, J and L). Normal looking lamellar bodies were also present (Fig. 7 F). Using ruthenium tetroxide after fixation, the typical lipid lamellae within lamellar bodies (Fig. 7 G), as well as the stacks of lipid lamellae representing extruded content of lamellar bodies in the transition zone between the last granular cell layer and the first cornified cell (Fig. 7 H), could be visualized. No difference in respect to the organization of the stacks or number of lamellae could be determined so far.

Increased fragility of cornified envelope (CE)

We prepared CEs from control and 12R-LOX$^{-/-}$ newborn epidermis to assess morphology and resistance to mechanical stress. Microscopic examination revealed no obvious structural abnormalities of the CEs isolated from mutant mice. Upon ultrasound treatment, however, the percentage of intact corneocytes from homozygous mutant mice decreased significantly ($P > 0.01$) faster with time, compared with CEs from wild-type and heterozygous littermates, indicating an increased fragility of the mutant CEs (Fig. 8).

Altered lipid composition

The structural anomalies in the skin of 12R-LOX–null mice indicated that defects in the lipid metabolism may be associated with the observed phenotype. It is well known that lipid constituents, such as free fatty acids, cholesterol, and ceramides, play an important role in epidermal barrier function. On the extracellular surface of the CE there is a covalently bound layer of very long chain ω-hydroxyceramides and ω-hydroxy-fatty acids, called the lipid envelope. The exact function of the lipid envelope still remains unclear, but there is evidence that interactions of protein-bound lipids with free intercellular lipids contribute to the patterned organization of the lamellae seen in EM (Madison, 2003). It has been shown that alterations in lipid composition of free or protein-bound lipids impair barrier function of the skin and lead to an increased TEWL (Meguro et al., 2000; Macheleidt et al., 2002). We thus determined the levels of these lipids in the skin of wild-type and mutant mice. The levels of total fatty acids,

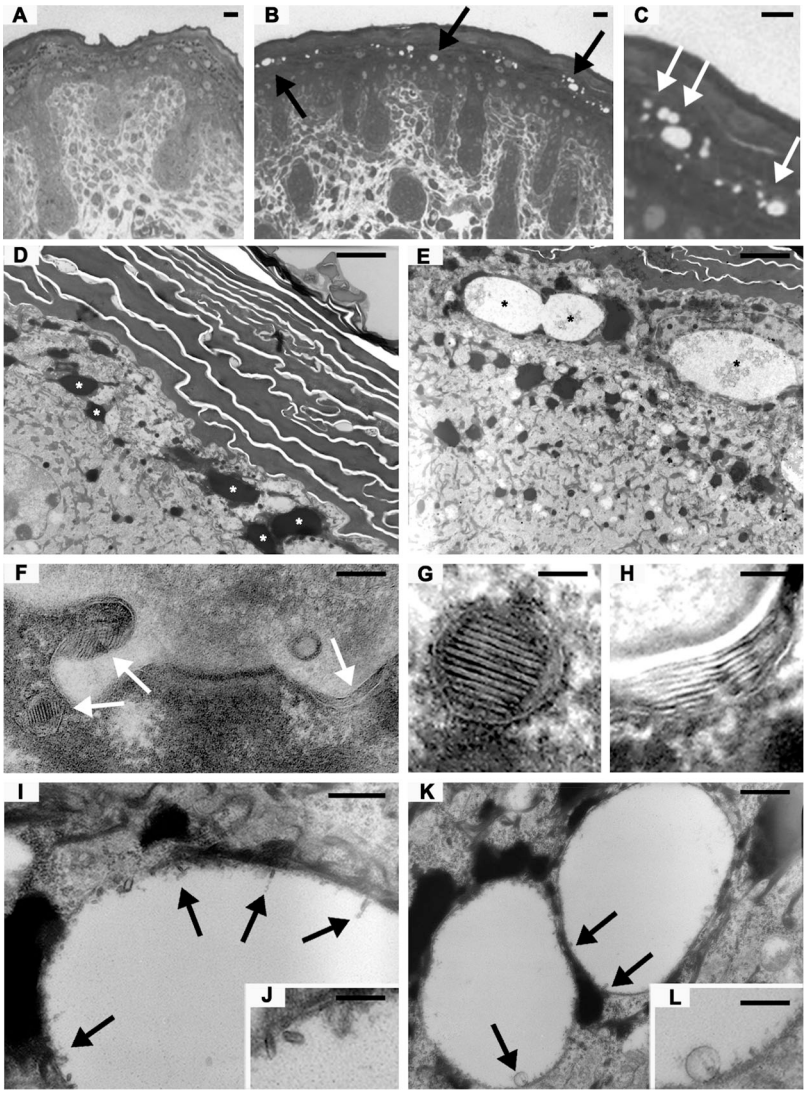

Figure 7. **Ultrastructural anomalies in 12R-LOX$^{-/-}$ mice.** (A–C) Methylene blue staining images of semithin sections from newborn dorsal skin of wild-type (A) and knockout mice (B and C). Arrows indicate irregular vesicular structures in the upper granular layers of the knockout skin. (D–L) Back skin of wild-type (D) and 12R-LOX$^{-/-}$ (E–L) mice was processed for transmission EM. (D) Normal horny and granular layer in wild-type epidermis. Asterisks depict keratohyalin granules. (E) Abnormal vesicular structures (asterisks) within granular layer. (F) Normal lamellar bodies (arrows) within granular layer. (G) Normal lamellar body; improved presentation of lamellae stacks by ruthenium tetroxide postfixation. (H) Improved visualization of lipid lamellae stacks between uppermost epidermal cell and first keratinized cell. (I and J) Membranous material resembling the content of lamellar bodies adheres to the marginal membrane of irregular vesicles (arrows). (K and L) Details of irregular vesicles; membranous material and small vesicle. Bars: (A–C) 10 μm; (D) 2.25 μm; (E) 3 μm; (F) 500 nm; (G and H) 50 nm; (I and J) 513/250 nm; (K and L) 500/200 nm.

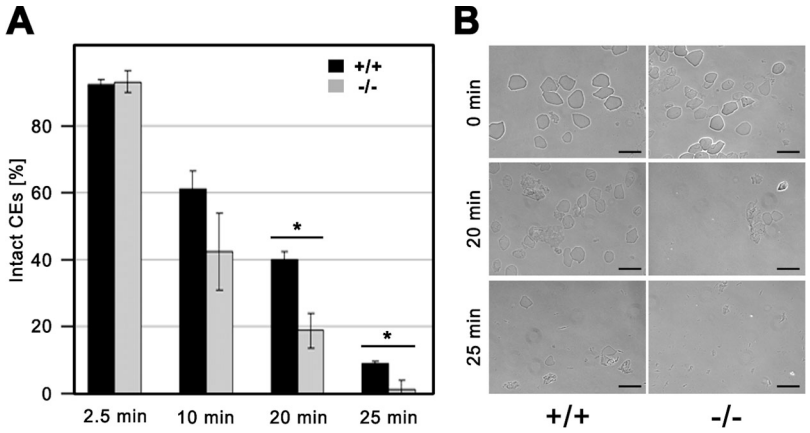

Figure 8. **Increased fragility of mutant CE.** CEs were isolated from 12R-LOX$^{-/-}$ and wild-type epidermis, and samples of 5×10^6 CEs in 0.5 ml extraction buffer were treated with ultrasound at 4°C. (A) At indicated time points, 5-μl aliquots were removed, and the percentage of intact CEs was determined with the hematocytometer. Data are presented as the mean ± the SD. *, $P < 0.01$. (B) Morphological appearance of wild-type and knockout CEs. In untreated CEs, no clear difference between knockout and control skin was observed. After 20 min of treatment, most mutant CEs were destroyed, whereas a large fraction of wild-type CEs were still intact. Shown is one of two independent experiments with similar results. Bars, 100 μm.

cholesterol, and total free ceramides were not substantially different between control and 12R-LOX–deficient mice (not depicted). In the free ceramide fraction, we found mainly ceramide EOS, NS, and NP, as well as two ceramide AS species (Fig. 9). These results are in accordance with previously published results (Doering et al., 1999, 2002). However, in the protein-bound fraction, five different species could be detected on HPTLC (B1–5). The exact identities of these species still have to be elucidated, but B4 is possibly ceramide OS. Significant differences were found in the subfractions of ester-bound lipids between wild-type and knockout mice. Whereas species B1 was found significantly increased, three other species (B2, B4, and B5) were almost completely absent in knockout epidermis (Fig. 9).

Discussion

We report the successful targeted disruption of *Alox12b* in mice, which reflects features of ARCI and shows that 12R-LOX has a crucial role in the establishment of the epidermal barrier.

The epidermis is a self-renewing stratified epithelium that serves as a protective barrier against mechanical, chemical, and biological insults; it is also a water-impermeable barrier that prevents excessive loss of body fluids. This function is critical for the survival of all terrestrial vertebrates and is established during late embryonic development. Identification of the molecular nature of the barrier is still under investigation. There is consent, however, that specialized structures in the stratum

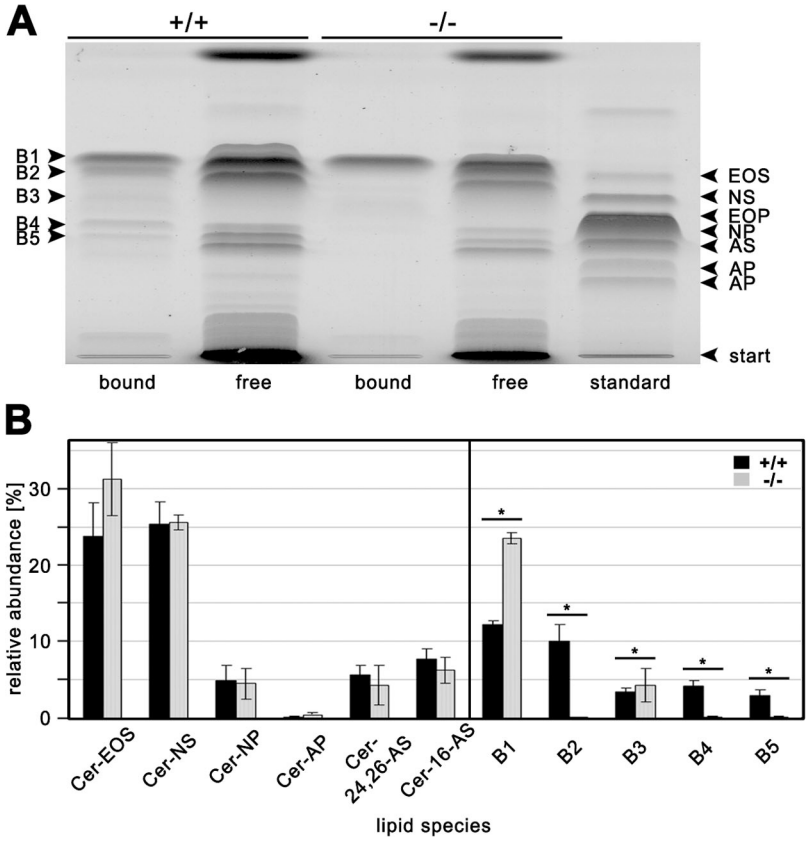

Figure 9. **Altered ceramide composition of 12R-LOX$^{-/-}$ epidermis.** Free and ester-linked epidermal lipids were extracted and separated using TLC. Ceramides are classified as suggested in previous works (Motta et al., 1993; Robson et al., 1994). B1–5 are lipids extracted after alkaline hydrolysis, most likely ester-linked epidermal lipids. (A) A representative TLC analysis of lipids extracted from wild-type and knockout epidermis. (B) Individual lipid levels quantified by densitometric analysis. Data are presented as the mean ± the SEM. $n = 3$. *, $P < 0.01$. Shown is one of two independent experiments with similar results.

corneum, the CE, and extracellular lipid lamellae, as well as tight junctions in the granular layers, play essential roles in the development of the skin barrier function (Tsuruta et al., 2002; Segre, 2003).

The stratum corneum is formed from granular cells during terminal differentiation as keratinocytes ascend from the proliferative cell type in the basal layer through the spinous and granular layers to end up as flat, dead corneocytes within the cornified layer. The CE is assembled underneath the plasma membrane by sequential incorporation and transglutaminase-mediated cross-linking of precursor proteins, followed by the covalent attachment of extracellular lipids. At the granular layer–stratum corneum interface, the lamellar bodies that are thought to be elements of the tubulovesicular TGN fuse with the cell membrane and extrude their contents to form a multilamellar lipid complex that fills most of the intercellular space.

Pathological abnormalities in the stratum corneum, with the subsequent breakdown of epidermal barrier function, are observed in various skin diseases, which are referred to as ichthyoses. The loss of barrier function can be caused by several defects in the molecular mechanisms involved in the proper assembly of the CE or the intercorneocyte lipids. Several defective genes have been identified in ichthyosiform skin disorders so far, including genes coding for CE components (keratins, loricrin, and filaggrin) and proteins involved in the assembly and protein turnover (transglutaminase 1 and LEKTI), and, most frequently, genes coding for enzymes involved in lipid metabolism (e.g., fatty aldehyde dehydrogenase, steroid sulfatase, glucocerebrosidase, ATP-binding cassette transporter, (for review see Richard, 2004). Recent studies from our group and others have linked inactivating mutations in the genes of 12R-LOX and eLOX-3 to the development of ARCI (Jobard et al., 2002; Eckl et al., 2005).

12R-LOX is a member of the LOX multigene family, exhibiting, among mammals, a unique R-stereospecificity of oxygen insertion. The enzyme is found almost exclusively in skin. In mouse epidermis, a predominant mRNA expression was observed in the differentiated keratinocytes (Sun et al., 1998; Heidt et al., 2000). By immunofluorescence analyses, we could now localize the 12R-LOX protein at the surface of the keratinocytes in the stratum granulosum, indicating a function in late epidermal differentiation. Interestingly, an almost identical expression pattern was observed for eLOX-3 (not depicted), suggesting a colocalization of both LOX in the plasma membranes of the stratum granulosum. The implication of 12R-LOX and eLOX-3 in ARCI has brought forth the concept that both enzymes function in the same metabolic pathway to convert arachidonic acid via 12R-HPETE to hepoxilin- and trioxilin-like metabolites that are critically involved in keratinocyte differentiation (Jobard et al., 2002; Eckl et al., 2005; Yu et al., 2005; Lefevre et al., 2006). As shown for enzymes of the leukotriene synthesis, which form multimeric complexes in the nuclear membrane (Mandal et al., 2004), a coordinated membrane organization of these two enzymes, probably together with other enzymes and/or accessory proteins, may be a prerequisite for full enzyme activity and the proper generation of the bioactive lipid products of the 12R-LOX–eLOX-3 pathway in skin.

Indeed, under cell-free conditions, the recombinant human 12R-LOX exhibits only low catalytic activity converting arachidonic acid to 12R-HPETE, whereas the mouse enzyme does not metabolize free arachidonic acid, but only esterified substrates, including arachidonic acid and linoleic acid methyl esters (Siebert et al., 2001). This has raised the question as to the nature of the endogenous substrate and the functional homology of the mouse and human enzyme (Krieg et al., 1999; Yu et al., 2005, 2006). The results of this paper demonstrate an essential role of 12R-LOX in the development of epidermal barrier function in mice, documenting a functional homology of the mouse and human enzyme in skin.

12R-LOX–deficient mice exhibited the most severe phenotype regarding water barrier dysfunction reported so far. All knockout mice died within 3–5 h after birth as a result of severe dehydration. The mice lost ~10% of their weight per hour. Other knockout mouse models with epidermal barrier defects, including mice deficient in KLF4 (Segre et al., 1999), claudin (Furuse et al., 2002), E-cadherin (Tunggal et al., 2005), LEKTI (Descargues et al., 2005), CAP1 (Leyvraz et al., 2005), and FATP4 (Herrmann et al., 2003), exhibited substantially less weight loss, resulting in a longer life span of the transgenic mice. Analyses of dye permeability and of TEWL clearly demonstrated a severely defective inward and outward epidermal barrier function in 12R-LOX–deficient mice, while the barrier function of tight junctions was unaffected. The knockout mice failed to develop a functional epidermal barrier, which was acquired in wild-type mice around E17. At this time point, expression of 12R-LOX, which starts in embryonic skin at E15.5, was shown to reach high levels that persists at later embryonic stages and in newborn skin (Sun et al., 1998).

Defective skin barrier function typically results in compensatory mechanisms involving epidermal hyperproliferation, hyperkeratosis, and/or parakeratosis, which are observed frequently in ichthyosiform human skin and various mouse models (Elias, 2004). 12R-LOX–deficient mice did not display such an obvious cutaneous phenotype, which may not develop because of the early neonatal lethality. In fact, markers of keratinocyte proliferation and terminal differentiation appeared to be unaffected, with the exception of filaggrin.

This late terminal differentiation marker is the result of a complex proteolytic processing of profilaggrin by several enzymes, including protein phosphatases, proteases, and protease inhibitors (Resing et al., 1984). Only mature filaggrin aggregates keratin filaments to form macrofibrils that crisscross the cornified cells of the stratum corneum, and it is an integral part of CE that contributes to its structural integrity. Thus, the decreased mechanical strength of CE from *Alox12b*$^{-/-}$ mice may be caused by the reduced profilaggrin processing. Furthermore, filaggrin monomers are degraded and provide free amino acids that, together with derivatives of amino acids and specific salts, constitute the natural moisturizing factor that is involved in the hydration of the stratum corneum (Rawlings et al., 1994). Thus, reduction of filaggrin monomers might explain the more densely packed stratum corneum, which could contribute to the impairement of the barrier function in the mutant mice. In fact, disturbance of the proteolytic profilaggrin processing by gene

inactivation has been shown to be associated with impairment of barrier function in several mouse models (Presland et al., 2000; List et al., 2002, 2003; Leyvraz et al., 2005; Descargues et al., 2005). In humans, lack of proteolytically processed filaggrin monomers caused by loss-of-function mutations have been shown to underlie ichthyosis vulgaris and discussed to be a major predisposing factor for atopic dermatitis (Sandilands et al., 2006; Smith et al., 2006).

An important component of the epidermal barrier is the arrangement of intra- and extracellular lipid accumulation in the stratum granulosum and stratum corneum, in particular the processing of intracellular lipids and the process of their extrusion into the intercellular space. Ultrastructural analysis revealed structural anomalies in the upper granular layers of the skin of 12R-LOX knockout mice that may reflect defects in the lipid metabolism associated with the observed phenotype. The features of the abnormalities are reminiscent of characteristic alterations found in a subgroup of ichthyosis congenital patients (Anton-Lamprecht, 1992). They include electron-lucent vesicles of variable size with lamellar structures reminiscent of the content of lamellar bodies adhering to the surrounding membrane. The appearance of these structures suggests that they may originate from defects in the assembly and/or extrusion of lamellar bodies, probably caused by aberrant lipid processing. Electron microscopic examination with ruthenium tetroxide postfixation to preserve lipid structure did not reveal major disturbances of the intercellular lipid lamellae. However, we presently cannot exclude more subtle local disturbances of these structures. Nevertheless, this analysis refers to a specific defect in lipid content and organization that may contribute to the barrier impairment observed in *Alox12b*$^{-/-}$ mice. Although the levels of total fatty acids, cholesterol, and free ceramides did not show substantial differences between control and mutant mice, we observed significant alterations in ester-bound lipids from *Alox12b*$^{-/-}$ mice. Ceramides covalently attached to involucrin and other CE peptides are major constituents of the cornified lipid envelope that surrounds the corneocyte and have been discussed to be critical components of the barrier function (Elias et al., 2000; Doering et al., 2002). The identity of the lipid species altered in the 12R-LOX–deficient epidermis remains to be elucidated.

It also remains to be established weather 12R-LOX is directly involved in the enzymatic lipid processing or in the generation of lipid metabolites that are involved in the regulation of lipid metabolism. It is of interest to note that the epoxyalcohol metabolites produced by the 12R-LOX–eLOX-3 pathway are able to transactivate peroxisome proliferator-activated receptors (PPARs; Yu, 2005). Recent studies provide evidence for a role of PPARs in the regulation of terminal keratinocyte differentiation, including lipid synthesis and processing (Di Poi et al., 2004; Elias, 2005). Moreover, it was recently reported that PPAR activators are able to accelerate permeability barrier recovery after acute barrier disruption (Man et al., 2006).

In summary, this study indicates that the 12R-LOX–eLOX-3 pathway plays a key role in the process of epidermal barrier acquisition by affecting lipid metabolism, as well as protein processing.

Materials and methods

Generation of 12R-LOX–deficient mice

Mouse genomic DNA for the targeting vector was cloned from a 129/ola mouse PAC library (clone RPCI-21 K13407Q2; obtained from P.J. de Jong and K. Osoegawa, Roswell Park Cancer Institute, Buffalo, NY). By using a 7.4-kb BamHI fragment and a 4.4-kb PCR-generated fragment containing exon 7–12, a homology region was cloned into pBluescript KS+ (Stratagene) that spanned from 226 nt upstream of exon 3 to 1,081 nt downstream of exon 11 (Krieg et al., 1999). A *tk/neo* selection cassette flanked by two loxP sites was inserted 230 bp upstream of exon 8, replacing a 222-bp AccI fragment; a third loxP site was inserted 84 bp downstream of exon 8, deleting a BamHI site (Fig. 1 A). The linearized targeting vector was electroporated into ES cells. Screening was done by PCR at both the 5′- and 3′-end using primer pairs consisting of one vector-specific primer and one endogenous *Alox12b*-specific primer located outside of the targeting region. The primers used were as follows: 5′-end screening, 5′-CCGTCGACCTCGACCAGCCTGTCTACA-3′ and 5′-CTGAGGCCAGAAGATCACAAGTTCAAG-3′; 3′-end screening, 5′-GAGGCATCCGGGGATCATAACTTCGTATA-3′ and 5′-CAGGTATAGTTCGCAAGCAGGTGG-3′. *Alox12b* gene targeting was further verified by Southern blot hybridization of BamHI-digested genomic DNA using 5′- and 3′-end probes flanking the recombination arms (Fig. 1 A). Two homologous recombinants were identified out of 300 analyzed. ES cells were injected into C57BL/6 blastocysts to generate chimeric mice, which were mated with C57BL/6 females. F1 heterozygotes (*Alox12b*$^{+/flox}$) were then crossed to 129S6. Mice were bred at the central animal facility of the German Cancer Research Center. All animals were kept under an artificial day/night rhythm and were fed standard food pellets (Altromin), with sterile water available ad libitum. The animal experiments were performed in accordance with the guidelines of the Arbeitsmeinschaft der Tierschutzbeauftragten in Baden-Württemberg (Officials for Animal Welfare) and were approved by the Regierrungspräsidum Karlsruhe, Germany.

To convert the targeted allele into a mutant allele structurally lacking the essential exon 8 of the *Alox12b* gene, F3 *Alox12b*$^{+/flox}$ heterozygotes were crossed with CMV-Cre transgenic mice exhibiting ubiquitous Cre expression (Schwenk et al., 1995). Complete excision of the resistance cassette and exon 8 in offspring mice was confirmed by Southern blot and PCR analyses (Fig. 1 C). Heterozygous mutant mice (*Alox12b*$^{+/-}$) were bred with 129S6, and their heterozygous offspring were intercrossed to obtain homozygous mutant mice (*Alox12b*$^{-/-}$). Genotyping was performed by PCR using 100 ng DNA isolated from tail and organs as a template and the primers ol1231 (5′-ACCCTCCCCTGCTGCTGTTGC-3′) and ol709 (5′-AGAGACCTCCCTTGTTGAGAAG-3′) to distinguish the 459-bp mutant allele band from the 1,075-bp wild-type band (Fig. 1 D).

RNA isolation and RT-PCR

Total RNA was isolated from epidermis as previously described (Kinzig et al., 1999) and mRNA was reverse transcribed with MuLV reverse transcriptase using the SuperScript II first strand synthesis system (Invitrogen). The resulting cDNA was subjected to PCR with the primer pairs ol230 (5′-CTGTGCCCCGATGTGCTTGCTG-3′) and ol709 (3′-AGAGACCTCCCTTGTTGAGAAG-5′) for 12R-LOX. As a control, β-actin cDNA was amplified as a housekeeping gene.

Antibodies

Rabbit polyclonal antipeptide antibodies against 12R-LOX and eLOX-3 have been previously described (Eckl et al., 2005). Mouse anti–12R-LOX mAb were raised using GST-12R-LOX fusion protein as immunogen. Other primary antibodies used were goat anti-actin (Santa Cruz Biotechnology), rabbit anti–Claudin-1, rabbit anti-occludin (both from Invitrogen), mouse anti-filaggrin (Monosan), rabbit anti-keratin 5, rabbit anti-keratin 10, rabbit anti-involucrin, and rabbit anti-Ki67 (all from CRP). Secondary antibodies used were Alexa Fluor 488 goat anti–mouse IgG (Invitrogen), CY3 anti–rabbit IgG (BD Biosciences), and anti–goat antibodies (Santa Cruz Biotechnology).

Epidermal protein extraction and Western blot analysis

Trunk epidermis of newborn mice was separated mechanically from the dermis after incubation for 30 s at 56°C in PBS. Epidermal proteins were extracted as described elsewhere (Tunggal et al., 2005; Leyvraz et al., 2005), and Western blot analysis was performed as previously described (Eckl et al., 2005).

Histological and immunofluorescence analysis

For light microscopic observation, samples were fixed for 24 h with 4% formalin in PBS, dehydrated in 70% ethanol, and embedded in paraffin.

5-μm sections were mounted on slides, dewaxed, rehydrated, and stained with hematoxylin and eosin. For methylene blue staining, skin was fixed with 1% glutaraldehyde for 24 h and embedded in epon. 1-μm sections were stained with methylene blue. For immunofluorescence microscopy, cryosections (3-μm thick) were fixed in acetone for 10 min at −20°C and permeabilized with 0.05% Triton X-100 in PBS and flushed with PBS. The slides were blocked in 1% BSA in PBS for 1 h and incubated with the primary antibody for 1 h. After washing three times (10 min each) in PBS, samples were incubated with a fluorescent dye coupled with antibody and Hoechst 33258 diluted in blocking buffer for 30 min and washed three times. Sections were embedded in mounting medium (DakoCytomation) and examined by light microscopy using a photomicroscope (Axioplan 2) with a 25× Plan-Neofluar objective (both Carl Zeiss MicroImaging, Inc.). Images were acquired with a high sensibility digital black/white AxioCam (Carl Zeiss MicroImaging, Inc.).

Preparation of CEs and sonication experiments

CEs were purified and sonicated at 4°C for various time points in a bath sonicator, as previously described (Koch et al., 2000).

Functional analyses of the epidermal barrier

To determine the rate of fluid loss, newborns were separated from their mother and kept at 37°C. The body weight was monitored every 30 min, until time of death of homozygous mutant mice. The rate of TEWL from the skin of newborn mice was determined by using a Tewameter (Courage + Khazaka). For penetration assays, backs of newborn mice were immersed in 1 mM Lucifer yellow in PBS at 37°C. After 1 h incubation, mice were killed and the skin was dissected out. Frozen sections were counterstained with propidium iodide and penetration of the dye was assessed by immunofluorescence microscopy.

Toluidine blue staining of mouse embryos

The developmental stage of mouse embryos was determined based on the assumption that fertilization occurred in the middle of the dark cycle the day before plugs were identified. The embryos were subjected to methanol dehydration and subsequent rehydration, as previously described (Koch et al., 2000), washed in PBS for 1 min, and stained for 30 min in 0.1% toluidine blue O/PBS. After destaining in PBS for 15 min, the embryos were photographed.

EM

All specimens were fixed for at least 2 h at room temperature in 3% glutaraldehyde solution in 0.1 M cacodylate buffer, pH 7.4, cut into pieces of ~1 mm^3, washed in buffer, postfixed for 1 h at 4°C in 1% osmium tetroxide or in 0.5% ruthenium tetroxide, rinsed in water, dehydrated through graded ethanol solutions, transferred into propylene oxide, and embedded in epoxy resin (Glycidether 100; Merck). Ultrathin sections were treated with uranyl acetate and lead citrate and examined with an electron microscope (EM 400; Philips).

Lipid analysis

Chemicals. Ceramide AS was purchased from Sigma-Aldrich. Ceramide NS was provided by Sederma, and ceramides EOS, EOP, NP, and AP were provided by Degussa.

Lipid extraction. Lipid extraction followed a previously described protocol (Doering et al., 1999) with slight modifications. In brief, epidermis homogenate was extracted twice, first overnight with chloroform (methanol 1:2 at room temperature) and second with 2 ml chloroform (methanol 2:1 for 1 h at room temperature). The organic layers of both extraction steps were combined, the solvent was removed using a Christ Speed-Vac Alpha RVC/Alpha 2–4 (Christ), and the residue was redissolved in 100 μl methanol/chloroform at a 1:1 ratio.

For recovery of protein-bound lipids, the pretreated pellet was incubated with 1 ml of 1 N NaOH in methanol at a ratio of 19:1, followed by extraction with 2 ml of chloroform for 1 h at 37°C. The organic layer was removed and washed with 3 ml of PBS–buffer; after phase separation, the solvent of the organic layer was evaporated in the Speed-Vac and the residue was redissolved in 100 μl methanol/chloroform at a ratio of 1:1. Lipid extracts were stored at −20°C until use.

Lipid HPTLC. Analysis of epidermal lipids by HPTLC followed a previously described protocol (Farwanah et al., 2002). In brief, 50 μl of a sample were applied on a prewashed TLC plate, together with reference lipids, using an Automatic TLC Sampler 4 (CAMAG). The development of the plates has been performed automatically using an AMD-2 apparatus (CAMAG). The AMD procedure used included a 17-step gradient of decreasing polarity, as previously described (Farwanah et al., 2002). After drying, the plates were sprayed with an aqueous solution of 10% $CuSO_4$ (wt/vol), 8% H_3PO_4 (vol/vol), and 5% methanol (vol/vol) using a ChromaJet DS20 (Sarstedt), charred in a drying oven at 180°C for 30 min, and, finally, scanned using a TLC Scanner 3 (CAMAG). Integration and quantification based on peak areas were performed using WinCATS software (CAMAG). Quantitative results for all ceramides were related to ceramide NP.

We thank Ina Kutschera, Dagmar Kucher, Brigitte Steinbauer, Nadine Krenzer, Mareen Neumann, and Cornelia Hasenknopf for excellent technical assistance. We are grateful to Peter Angel and Marina Schorpp-Kistner for participating in the targeting strategy and for helpful advice regarding embryo dissection. We thank Holger M. Reichardt for providing the tk/neo selection cassette; Ulrich Kloz and Frank van der Hoeven for carrying out the blastocyst injections; Lutz Langbein, Hans-Jürgen Stark, and Dirk Breitkreutz for providing antibodies and helpful advice with the immunofluorescence; Iris Helfrich for help with TEWL measurements; and Hans Christian Hennies for supporting the generation of the 12R-LOX mAb.

This work was supported by grants from the Deutsche Forschungsgemeinschaft (KR 905/5-1 and KR 905/6-1) and by a financial gift from the Selbsthilfe Ichthyose e.V.

Submitted: 20 December 2006
Accepted: 6 March 2007

References

Anton-Lamprecht, I. 1992. The skin. *In* Diagnostic Ultrastructure of Non-Neoplastic Diseases. J.M. Papdimitriou, D.W. Henderson, and V. Spagnolo, editors. Churchill-Livingstone. pp. 449–550.

Boeglin, W.E., R.B. Kim, and A.R. Brash. 1998. A 12R-lipoxygenase in human skin: mechanistic evidence, molecular cloning, and expression. *Proc. Natl. Acad. Sci. USA*. 95:6744–6749.

Brash, A.R. 1999. Lipoxygenases: occurrence, functions, catalysis, and acquisition of substrate. *J. Biol. Chem.* 274:23679–23682.

Descargues, P., C. Deraison, C. Bonnart, M. Kreft, M. Kishibe, A. Ishida-Yamamoto, P. Elias, Y. Barrandon, G. Zambruno, A. Sonnenberg, and A. Hovnanian. 2005. Spink5-deficient mice mimic Netherton syndrome through degradation of desmoglein 1 by epidermal protease hyperactivity. *Nat. Genet.* 37:56–65.

Di Poi, N., L. Michalik, B. Desvergne, and W. Wahli. 2004. Functions of peroxisome proliferator-activated receptors (PPAR) in skin homeostasis. *Lipids*. 39:1093–1099.

Doering, T., W.M. Holleran, A. Potratz, G. Vielhaber, P.M. Elias, K. Suzuki, and K. Sandhoff. 1999. Sphingolipid activator proteins are required for epidermal permeability barrier formation. *J. Biol. Chem.* 274:11038–11045.

Doering, T., H. Brade, and K. Sandhoff. 2002. Sphingolipid metabolism during epidermal barrier development in mice. *J. Lipid Res.* 43:1727–1733.

Eckl, K.M., P. Krieg, W. Kuster, H. Traupe, F. Andre, N. Wittstruck, G. Furstenberger, and H.C. Hennies. 2005. Mutation spectrum and functional analysis of epidermis-type lipoxygenases in patients with autosomal recessive congenital ichthyosis. *Hum. Mutat.* 26:351–361.

Elias, P.M. 2004. The epidermal permeability barrier: from the early days at Harvard to emerging concepts. *J. Invest. Dermatol.* 122:xxxvi–xxxix.

Elias, P.M. 2005. Stratum corneum defensive functions: an integrated view. *J. Invest. Dermatol.* 125:183–200.

Elias, P.M., M. Fartasch, D. Crumrine, M. Behne, Y. Uchida, and W.M. Holleran. 2000. Origin of the corneocyte lipid envelope (CLE): observations in harlequin ichthyosis and cultured human keratinocytes. *J. Invest. Dermatol.* 115:765–769.

Farwanah, H., R. Neubert, S. Zellmer, and K. Raith. 2002. Improved procedure for the separation of major stratum corneum lipids by means of automated multiple development thin-layer chromatography. *J. Chromatogr. B Analyt. Technol. Biomed. Life Sci.* 780:443–450.

Furuse, M., M. Hata, K. Furuse, Y. Yoshida, A. Haratake, Y. Sugitani, T. Noda, A. Kubo, and S. Tsukita. 2002. Claudin-based tight junctions are crucial for the mammalian epidermal barrier: a lesson from claudin-1-deficient mice. *J. Cell Biol.* 156:1099–1111.

Hardman, M.J., P. Sisi, D.N. Banbury, and C. Byrne. 1998. Patterned acquisition of skin barrier function during development. *Development*. 125:1541–1552.

Heidt, M., G. Fürstenberger, S. Vogel, F. Marks, and P. Krieg. 2000. Diversity of murine lipoxygenases: Identification of a subfamily of epidermal isoenzymes exhibiting a differentiation-dependent mRNA expression pattern. *Lipids*. 35:701–707.

Herrmann, T., F. van der Hoeven, H.J. Grone, A.F. Stewart, L. Langbein, I. Kaiser, G. Liebisch, I. Gosch, F. Buchkremer, W. Drobnik, et al. 2003. Mice with targeted disruption of the fatty acid transport protein 4 (Fatp 4, Slc27a4) gene show features of lethal restrictive dermopathy. *J. Cell Biol.* 161:1105–1115.

Jobard, F., C. Lefevre, A. Karaduman, C. Blanchet-Bardon, S. Emre, J. Weissenbach, M. Ozguc, M. Lathrop, J.F. Prud'homme, and J. Fischer. 2002. Lipoxygenase-3 (ALOXE3) and 12(R)-lipoxygenase (ALOX12B) are mutated in non-bullous congenital ichthyosiform erythroderma (NCIE) linked to chromosome 17p13.1. *Hum. Mol. Genet.* 11:107–113.

Kinzig, A., M. Heidt, G. Fürstenberger, F. Marks, and P. Krieg. 1999. cDNA cloning, genomic structure and chromosomal localization of a novel murine epidermis-type lipoxygenase. *Genomics*. 58:158–164.

Koch, P.J., P. A. de Viragh, E. Scharer, D. Bundman, M.A. Longley, J. Bickenbach, Y. Kawachi, Y. Suga, Z. Zhou, M. Huber, et al. 2000. Lessons from loricrin-deficient mice: compensatory mechanisms maintaining skin barrier function in the absence of a major cornified envelope protein. *J. Cell Biol.* 151:389–400.

Krieg, P., M. Siebert, A. Kinzig, R. Bettenhausen, F. Marks, and G. Furstenberger. 1999. Murine 12(R)-lipoxygenase: functional expression, genomic structure and chromosomal localization. *FEBS Lett.* 446:142–148.

Krieg, P., F. Marks, and G. Furstenberger. 2001. A gene cluster encoding human epidermis-type lipoxygenases at chromosome 17p13.1: cloning, physical mapping, and expression. *Genomics*. 73:323–330.

Krieg, P., M. Heidt, M. Siebert, A. Kinzig, F. Marks, and G. Furstenberger. 2002. Epidermis-type lipoxygenases. *Adv. Exp. Med. Biol.* 507:165–170.

Lefevre, C., B. Bouadjar, V. Ferrand, G. Tadini, A. Megarbane, M. Lathrop, J.F. Prud'homme, and J. Fischer. 2006. Mutations in a new cytochrome P450 gene in lamellar ichthyosis type 3. *Hum. Mol. Genet.* 15:767–776.

Leyvraz, C., R.P. Charles, I. Rubera, M. Guitard, S. Rotman, B. Breiden, K. Sandhoff, and E. Hummler. 2005. The epidermal barrier function is dependent on the serine protease CAP1/*Prss8*. *J. Cell Biol.* 170:487–496.

List, K., C.C. Haudenschild, R. Szabo, W. Chen, S.M. Wahl, W. Swaim, L.H. Engelholm, N. Behrendt, and T.H. Bugge. 2002. Matriptase/MT-SP1 is required for postnatal survival, epidermal barrier function, hair follicle development, and thymic homeostasis. *Oncogene*. 21:3765–3779.

List, K., R. Szabo, P.W. Wertz, J. Segre, C.C. Haudenschild, S.Y. Kim, and T.H. Bugge. 2003. Loss of proteolytically processed filaggrin caused by epidermal deletion of Matriptase/MT-SP1. *J. Cell Biol.* 163:901–910.

Macheleidt, O., H.W. Kaiser, and K. Sandhoff. 2002. Deficiency of epidermal protein-bound omega-hydroxyceramides in atopic dermatitis. *J. Invest. Dermatol.* 119:166–173.

Madison, K.C. 2003. Barrier function of the skin: "la raison d'etre" of the epidermis. *J. Invest. Dermatol.* 121:231–241.

Man, M.Q., E.H. Choi, M. Schmuth, D. Crumrine, Y. Uchida, P.M. Elias, W.M. Holleran, and K.R. Feingold. 2006. Basis for improved permeability barrier homeostasis induced by PPAR and LXR activators: liposensors stimulate lipid synthesis, lamellar body secretion, and post-secretory lipid processing. *J. Invest. Dermatol.* 126:386–392.

Mandal, A.K., J. Skoch, B.J. Bacskai, B.T. Hyman, P. Christmas, D. Miller, T.T. Yamin, S. Xu, D. Wisniewski, J.F. Evans, and R.J. Soberman. 2004. The membrane organization of leukotriene synthesis. *Proc. Natl. Acad. Sci. USA*. 101:6587–6592.

Meguro, S., Y. Arai, Y. Masukawa, K. Uie, and I. Tokimitsu. 2000. Relationship between covalently bound ceramides and transepidermal water loss (TEWL). *Arch. Dermatol. Res.* 292:463–468.

Motta, S., M. Monti, S. Sesana, R. Caputo, S. Carelli, and R. Ghidoni. 1993. Ceramide composition of the psoriatic scale. *Biochim. Biophys. Acta*. 1182:147–151.

Presland, R.B., D. Boggess, S.P. Lewis, C. Hull, P. Fleckman, and J.P. Sundberg. 2000. Loss of normal profilaggrin and filaggrin in flaky tail (ft/ft) mice: an animal model for the filaggrin-deficient skin disease ichthyosis vulgaris. *J. Invest. Dermatol.* 115:1072–1081.

Rawlings, A.V., I.R. Scott, C.R. Harding, and P.A. Bowser. 1994. Stratum corneum moisturization at the molecular level. *J. Invest. Dermatol.* 103:731–741.

Resing, K.A., K.A. Walsh, and B.A. Dale. 1984. Identification of two intermediates during processing of profilaggrin to filaggrin in neonatal mouse epidermis. *J. Cell Biol.* 99:1372–1378.

Richard, G. 2004. Molecular genetics of the ichthyoses. *Am. J. Med. Genet. C. Semin. Med. Genet.* 131C:32–44.

Robson, K.J., M.E. Stewart, S. Michelsen, N.D. Lazo, and D.T. Downing. 1994. 6-Hydroxy-4-sphingenine in human epidermal ceramides. *J. Lipid Res.* 35:2060–2068.

Sandilands, A., G.M. O'Regan, H. Liao, Y. Zhao, A. Terron-Kwiatkowski, R.M. Watson, A.J. Cassidy, D.R. Goudie, F.J. Smith, W.H. McLean, and A.D. Irvine. 2006. Prevalent and rare mutations in the gene encoding filaggrin cause ichthyosis vulgaris and predispose individuals to atopic dermatitis. *J. Invest. Dermatol.* 126:1770–1775.

Schwenk, F., U. Baron, and K. Rajewsky. 1995. A cre-transgenic mouse strain for the ubiquitous deletion of loxP-flanked gene segments including deletion in germ cells. *Nucleic Acids Res.* 23:5080–5081.

Segre, J. 2003. Complex redundancy to build a simple epidermal permeability barrier. *Curr. Opin. Cell Biol.* 15:776–782.

Segre, J.A., C. Bauer, and E. Fuchs. 1999. Klf4 is a transcription factor required for establishing the barrier function of the skin. *Nat. Genet.* 22:356–360.

Siebert, M., P. Krieg, W.D. Lehmann, F. Marks, and G. Furstenberger. 2001. Enzymic characterization of epidermis-derived 12-lipoxygenase isoenzymes. *Biochem. J.* 355:97–104.

Smith, F.J., A.D. Irvine, A. Terron-Kwiatkowski, A. Sandilands, L.E. Campbell, Y. Zhao, H. Liao, A.T. Evans, D.R. Goudie, S. Lewis-Jones, et al. 2006. Loss-of-function mutations in the gene encoding filaggrin cause ichthyosis vulgaris. *Nat. Genet.* 38:337–342.

Sun, D., M. McDonnell, X.S. Chen, M.M. Lakkis, H. Li, S.N. Isaacs, S.H. Elsea, P.I. Patel, and C.D. Funk. 1998. Human 12(R)-lipoxygenase and the mouse ortholog. Molecular cloning, expression, and gene chromosomal assignment. *J. Biol. Chem.* 273:33540–33547.

Traupe, H. 1989. The lamellar ichthyoses. *In* The Ichthyoses: A Guide to Clinical Diagnosis, Genetic Counseling, and Therapy. Springer, Berlin. pp. 111–134.

Tsuruta, D., K.J. Green, S. Getsios, and J.C. Jones. 2002. The barrier function of skin: how to keep a tight lid on water loss. *Trends Cell Biol.* 12:355–357.

Tunggal, J.A., I. Helfrich, A. Schmitz, H. Schwarz, D. Gunzel, M. Fromm, R. Kemler, T. Krieg, and C.M. Niessen. 2005. E-cadherin is essential for in vivo epidermal barrier function by regulating tight junctions. *EMBO J.* 24:1146–1156.

Yu, Z. 2005. Discovery of a novel lipoxygenase pathway in skin. PhD thesis. Vanderbilt University, Nashville, TN.

Yu, Z., C. Schneider, W.E. Boeglin, L.J. Marnett, and A.R. Brash. 2003. The lipoxygenase gene ALOXE3 implicated in skin differentiation encodes a hydroperoxide isomerase. *Proc. Natl. Acad. Sci. USA*. 100:9162–9167.

Yu, Z., C. Schneider, W.E. Boeglin, and A.R. Brash. 2005. Mutations associated with a congenital form of ichthyosis (NCIE) inactivate the epidermal lipoxygenases 12R-LOX and eLOX3. *Biochim. Biophys. Acta*. 1686:238–247.

Yu, Z., C. Schneider, W.E. Boeglin, and A.R. Brash. 2006. Human and mouse eLOX3 have distinct substrate specificities: Implications for their linkage with lipoxygenases in skin. *Arch. Biochem. Biophys.* 455:188–196.